An Acad Bras Cienc (2024) 96(3): e20231153 DOI 10.1590/0001-3765202420231153
Anais da Academia Brasileira de Ciências | *Annals of the Brazilian Academy of Sciences*
Printed ISSN 0001-3765 I Online ISSN 1678-2690
www.scielo.br/aabc | www.fb.com/aabcjournal

ENGINEERING SCIENCES

An investigation on the physical properties of cementitious pastes modified with low dosage of waste glass powder and silica fume

ANDRÉ L.S. PATRIOTA, FILIPE B.M. BARROS, ARNALDO M.P. CARNEIRO & PEDRO L. GUZZO

Abstract: Portland cement (PC) production is among the industrial activities that most emit harmful gases. Its replacement to green binders turns into a timely issue to face the global restrictions due to climate changes. In this study, some properties of cementitious pastes prepared with waste packing glass powder (GP) and silica fume (SF) were characterized in line with a prefixed alkaline equivalent limit. These materials were obtained in Northeastern Brazil. Grinding operations used to produce GP into four size ranges ([45-75] µm, < 45 µm; [25-45] µm, < 25 µm) were disclosed. X ray diffraction showed that GP and SF substitutions did not change the hydration products commonly observed in PC pastes. The portlandite content measured with thermogravimetry was affected by GP size in both unitary and binary substitutions. The compressive strength measured after 56 days of curing was dependent on portlandite and void index contents measured in hardened pastes. Scanning electron microscopy coupled to energy dispersive spectroscopy were useful to show the effect of the particle size on the pozzolanic activity. It was found that 5% of PC replacement for GP < 25 µm was enough to raise the compressive strength by ~5%. For binary substitution, the strength increasing was ~ 20 %. The collectors of solid residues are the main players of waste glass recycling in Brazil. It is expected that the results of this study contribute to take out these workers from the fringes of the citizenship.

Key words: glass powdering, silica fume, alkaline equivalent limit, glass recovery, compressive strength, microstructural analysis.

INTRODUCTION

The manufacturing process of Portland cement (PC) is one of the largest emitters of CO_2 into the atmosphere. Approximately 5-6 % of the anthropic CO_2 emissions is originated from gray and white cement industries (Ali et al. 2011, GCCA 2020). For a long time, large sums of supplementary cementitious materials (SCM) such as silica fume, blast-furnace slag, fly ash and calcined clays are being used in concrete either in blended cements or added separately in the concrete mixture (Lothenbach et al. 2011, Suraneni & Weiss 2017, Metha & Ashish 2020). SCM comprehend all solid ingredients that contribute to hydraulic and pozzolanic reactions during concrete maturation and, consequently, influencing its properties and durability. SCM are also those ingredients that contribute to reduce the consumption of non-renewable resources like limestone and dolostone - the carbonate rocks showing calcite ($CaCO_3$) and dolomite ($CaMg(CO_3)_2$) as major minerals, respectively, used in cement industry. In this century, the search for alternative supplementary cementitious materials (ASCM) is rapidly increasing. Fine particles of soda-lime glass obtained from food and beverage packing glass is

one of the most attractive ASCM due to its high content of amorphous silica, approximately 70%, and its broad availability worldwide (Federico & Chidiac 2009, Jani & Hogland 2014, Metha & Ashish 2020).

In Brazil, the 5th producer of urban solid residues in the world, approximately 570 thousand tons of waste soda-lime glass were recovered through selective collection between 2014 and 2017 (MMA-SNIR 2020). The Brazilian Northeast macro-region (NE) in particular, with approximately 57 million inhabitants, has a significant number of small companies of recycling glass thank to the contribution of *carroceiros*: the collectors of all kinds of solid residues struggling for their subsistence along the night streets with pushcarts. For instance, the mensal revenue of a collector working in the metropolitan region of Recife (PE) is around 100 USD (Oliveira et al. 2022). On the other hand, NE has important economic activities related to carbonate rocks mining as well as cement manufacturing and building construction. Unfortunately, these activities are far to be linked one each other on a way to boost a well-being state for the whole society. According to the survey carried out by Oliveira et al. (2022), the *carroceiros* of Recife (PE) are aware about the importance of their work for the whole recycling process of solid residues. Containers for waste glass storing is rare or still inexistent in the public corners of the metropolitan region of Recife. The survey also revealed that the high inhomogeneity of the residues is the second main problem. The first one is the extremely low financial return. Thus, further efforts from the engineering researchers is timely and decisive to gauge the technical feasibility of using waste glass powdering as ASCM in the Brazilian NE.

To achieve the performance of mortars and concretes usually obtained with PC blended with typical SCM, the physical properties and microstructure of cementitious pastes prepared with glass powders have been extensively investigated (e.g., Shao et al. 2000, Ismail & Al-Hashmi 2009, Idir et al. 2011, Matos & Coutinho 2012, Khrimi et al. 2013, Carsana et al. 2014, Du & Tan 2014, 2017, Afshinnia & Rangaraju 2015, You et al. 2021). In summary, these studies pointed to a rise in workability of fresh pastes and a strengthening on the mechanical properties and durability of concrete slabs cast with glass powder (GP) with particle size < 50 μm. Numerous works reported that the pozzolanic reaction in concretes prepared with fine GP occurs at lower rates compared to ordinary PC samples. Cement-GP substitution causes a decrease in compressive strength during early curing, but it increases for prolonged ages. However, the effect of single constituents on the pozzolanic reactions involving GP and the typical products of clinker hydration such as calcium-silicon-hydrates (C-S-H) and portlandite ($Ca(OH)_2$) has not been fully clarified due to the high complexity of these reactions. As known, the alkali (Na and K) content plays a crucial role in gel production due alkali-silica reaction (ASR) and remains one of the main concerns to employ cullet glass in building constructions (Federico & Chidiac 2009, Omran et al. 2017, ASTM 2020). Although not well understood, there is a consensus that glass particle size play an important role in ASR (Shi et al. 2005, Singh et al. 2016, Metha & Ashish 2020). Coarse glass fragments used as aggregates in concretes cast with ordinary PC shows intense reactivity with alkali in pore solution (Afshinnia & Rangaraju 2016). The control of ASR in concretes prepared with GP < 100 μm have also been reported (Idir et al. 2011, Afshinnia & Rangaraju 2015, Zheng 2016). Even though, the main body of the investigations were performed using GP substitution varying from 10 up to 30 % (by weight) without considering the alkali equivalent limit of the whole mixture. In addition, the acceptance of GP in cement and concrete industries is also limited by the absence of technical and sustainable indicators about unitary operations devoted to processing commingled glass (grinding and screening). Since fine grinding in industrial scale is a high-energy consumption

operation (Fuerstenau & Abouzeid 2002, Zhang et al. 2007, You et al. 2021), additional efforts to design the production of silica powders in controlled laboratory conditions can be helpful to assess the feasibility of glass cullet comminution for the purpose of ASCM.

The role of GP substitution in association with another SCM was considered in a smaller number of studies. Analyzing the effect of GP, quartz particle (QP), and silica fume (SF) on ultrahigh performance concrete (UHPC), Vaitkevičius et al. (2014) observed that GP accelerates the hydration process by increasing the dissolution rate of cement whereas SF consumes five times more portlandite compared to GP. An increase in more than 20 % in the compressive strength was observed when binary substitutions of GP and SF were used instead of GP and QP attesting the high reactivity of amorphous silica. Kamali & Ghahremaninezhad (2016) investigated the hydration and the pozzolanic reactivity in cement pastes modified with calcium-aluminum oxide (57.5 % SiO_2) and soda-lime (63.3 % SiO_2) GP with fine particle size (< 38 μm) and fly ash (54 % SiO_2). These authors concluded that GP enhances the hydration and the pozzolanic reactivity contributing to the pore refinement of the microstructure in comparison to the cement pastes modified with fly ash. On its turn, aiming to investigate the hydrothermal behavior of concretes prepared with high dosages of GP (20 and 30 wt%) and SF (5 wt%), Boukhelf et al. (2021) reported that these substitutions decrease the compressive strength of hardened concrete after 28 and 91 days. GP as a secondary replacement in cement paste has rarely been reported compared to concrete and mortar (Mehta & Ashish 2020). The microstructural analysis of unitary and binary substitutions in cement pastes can be more enlightening if one considers the absence of sand (mortar) and sand and aggregate (concrete) in the system to be studied.

The aim of this study was to investigate the properties of fresh and hardened pastes prepared with grey Portland cement mixed with small dosages of fine glass powder and silica fume to be in line with an alkaline equivalent limit < 1.5 %. The procedures used for powdering, screening, and blending were disclosed to encourage the construction industry and the glass recycling companies established in the Brazilian NE to employ such technical outcomes. The content of substitutions based on the alkaline equivalent limit and the adjustment of particle size ranges were the main concerns of this study. The workability of fresh pastes was estimated with a consistence index based on flow table tests. Structural and microstructural features of hardened pastes were assessed using X ray diffraction, thermal analysis and scanning electron microscopy coupled to energy dispersive spectroscopy. Among the properties investigated, the void index and the portlandite consumption were the most important parameters defining the compressive strength of pastes aged for 56 days. The influence of the glass particle size on the pozzolanic reactivity was discussed considering microscopic features observed in hardened pastes cast with unitary and binary replacements.

MATERIALS AND METHODS

Binders: provenance, grinding, characterization

The Portland cement identified as type V according with the ABNT NBR 16697:2018 standard, which is equivalent to the ASTM type I, was used in this study. This cement, labelled here as PCV, is manufactured by *CSN Alhandra – Cimento Elizabeth* (Alhandra, PB) and it is available throughout the NE Region. It was used to prepare the cementitious pastes containing low concentrations of glass powder (GP) and silica fume (SF). The silica fume (SF) was purchased from a regular supplier of NE. It was used in the

as-received condition. Beverage packaging waste glass was collected from the stockpile of a recycling company in Recife (PE) named *Fausto Soluções Ambientais Ltda*. Approximately 30 kg of colorless, green, and amber samples were cleaned using a 10% HNO_3 solution and household detergents. After drying in the sun, each sample was crushed by manual hammering to produce fragments < 45 mm and then mixed in the same proportion by weight (wt). Although indispensable for glass makers, the separation of packing glass by color is not essential for cement replacement since only slight differences are observed in the chemical composition of soda-lime glass depending on its color (Park et al. 2004, Mohajerani et al. 2017). Bignozzi et al. (2015) analyzed the effect of glass chemical composition on the compressive strength and the portlandite content of cement compounds blended with glass particles derived from tableware, cathode ray tube, fluorescent lamps and packing glass with unknow colors. The authors concluded that the higher concentration of NaOeq+PbO and the lower concentration of CaO+MgO in the fluorescent lamp glass composition caused a high degree of Na dissolution during the gel formation, which may explain the lower mechanical strength of the cement mortar prepared with 25 wt% of this waste in comparison to the other wastes. Thus, the use of mixed glass cullet for SCM purpose permits to recycle significant volumes of waste packing glass that are not functional to glass makers without separation by color.

The grinding and screening operations were carried out in two stages to produce four size fractions of glass powder (GP), as follows: (i) stage I: [45-75] µm and < 45 µm; (ii) stage II: [25-45] µm and < 25 µm. The procedure designed for grinding and screening cycles are shown in Fig. 1. The specifications of the laboratory ball mill are shown in Table I. The time elapsed for grinding and screening operations are detailed in Table II. As noted, the elapsed time to achieve the entire GP production is considerably high. The reasons for such time consumption are briefly addressed as follows. Feed and discharge processes during griding and screening operations were entirely carried

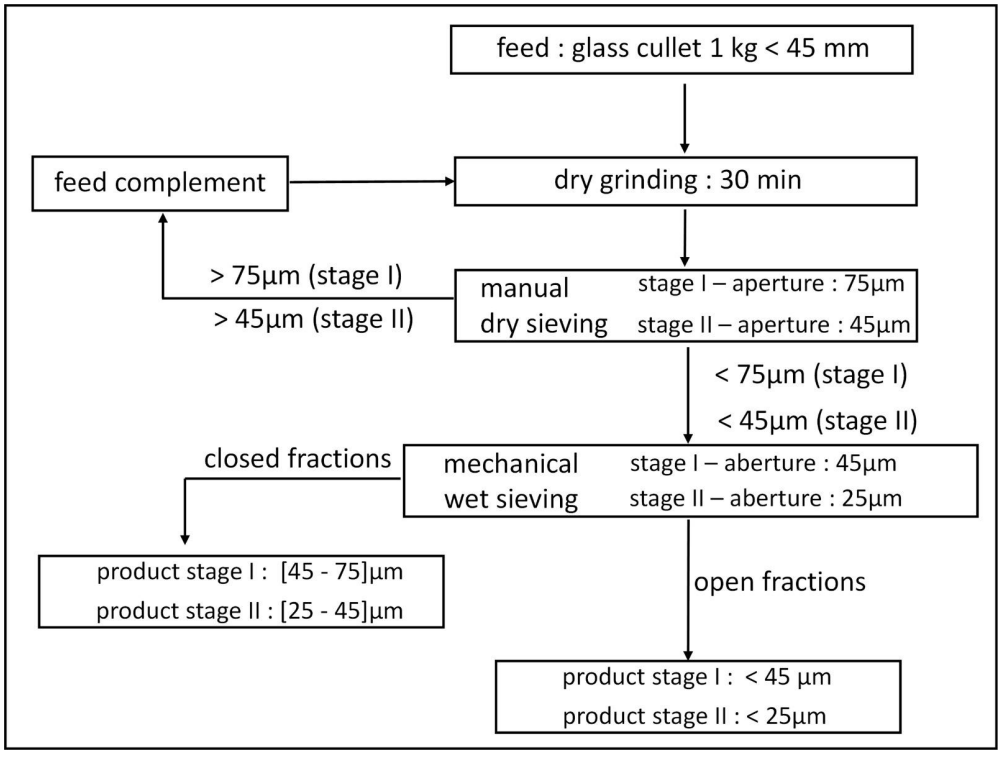

Figure 1. Diagram illustrating the steps designed to produce fine powders from waste packing glass (WPG) using hand-operated equipment. The procedure was executed two times (stages I and II).

out by hand. Significant time (and energy) consumption can be saved if the designed protocol (Fig. 1) is automated and customized for industrial applications. The low milling efficiency of fine (< 100 μm) grinding using standard ball mills under dry condition is another weakness of the designed protocol for industrial application. As known, interparticle agglomeration and cushioning effects are the main drawbacks of fine dry grinding with ball mill types (Austin & Bagga 1981, Guzzo et al. 2020). Previously, comparing the time performance to obtain ultrafine (< 10 μm) quartz particles free from agglomeration, it was concluded that the grinding efficiency of a 2-inch air jet mill was considerably higher than the efficiency of a planetary ball mill working at 300 rpm (Soares & Guzzo 2019). For the present study, dry grinding was chosen to avoid substantial modifications in the original reactivity of glass particle surfaces. Considering the size of glass cullet, a suitable alternative to carry out glass powdering would be to use two machines: ball mill and air-jet mill.

Particle size distribution (PSD) was measured using laser light scattering with a Malvern Mastersizer 2000 equipment. The measurements were performed with distilled water using the Hydro 2000 accessory. The PSD curve of each sample was the average of a sequence of three measurements. The characteristic diameters corresponding to 10 % (d_{10}), 50 % (d_{50}) and 90 % (d_{90}) of passing material were obtained from PSD curves. The specific surface area (SSA) was calculated using the Sauter diameter (Guzzo et al. 2020). The heterogeneity of the PSD was estimated using the d_{90}/d_{10} ratio. These parameters are summarized in Table III. For comparison, the particle size parameters determined for glass fragments used as feed for the ball mill, SF and PCV are also shown.

X-ray fluorescence (XRF) spectrometry was used to determine the chemical composition of the binders. The measurements were carried out with a PANalytical AXIOS mAX spectrometer equipped with a Rh tube. The quantitative analysis of the oxide concentrations was carried out using the method of calibration curves obtained with reference materials. For this, beads were produced at 1080 °C using lithium tetraborate and metaborate and ammonium iodide as fluxes, in a 1:4 ratio (sample:flux). The loss on ignition tests were carried out in an oven at 950 °C for 1 h. Table IV shows

Table I. Specifications of the pebble mill used to grind waste packing glass with top size < 45 mm.

characteristic	specification
mill chamber	porcelain; 3 L; diameter: 215 mm; length: 175 mm;
nominal power and rotation	880 W; 68 rpm
grinding media (pebbles)	alumina: 59 balls (< 35 mm);42 cylpebs (10x45 mm)
charge ratio	30 % (4650 g)
grinding condition	dry

Table II. Time consumption and production rates of fine powdering from waste packing glass.

stage	grinding time (h)	screening time (h)	size fraction	reduction factor*	production (g)	production rate (g/h)
I	80	80	[45-75] μm	180	4100	42.5
			< 45 μm	250	2700	
II	100	20	[25-45] μm	490	1200	26.7
			< 25 μm	840	2000	

*** calculated from d_{50} diameters shown in Table III.**

the major constituents found in each binder. The values for GP correspond to the average of the oxide concentrations measured for two samples ([45-75] μm and < 45 μm). The alkaline equivalent was calculated according to ASTM C1778 standard (2020). It was observed that the chemical composition for GP mixture shown in Table IV is in satisfactory agreement with the values reported for soda-lime glasses (Park et al. 2004, Bignozzi et al. 2015, Mohajerani et al. 2017, Alvarenga et al. 2019).

Fresh pastes: composition, preparation, consistency

The cementitious pastes were prepared replacing 5 wt% of PCV for GP and/or SF. The binary mixtures were formulated considering the alkaline equivalent (*AE*) of each supplementary material. The limit for available alkalis (*LAA*) for the binary replacement (GP+SF) was set at 1.5 wt% . This limit was defined considering the deleterious effect of excessive concentrations of Na_2O and K_2O in concrete reported in numerous studies (e.g. see Lothenbach et al. 2011, Kumar-Mehta & Monteiro 2014) as well as in technical standards specifying the alkaline limit for cement – silica fume substitutions (ABNT NBR 12653 2014, ASTM C1778 2020). Connecting *LAA* with the alkaline equivalents of glass powder (AE_{GP}), silica fume (AE_{SF}) and the total weight of the binary mixture (W_T), the weight of glass powder (W_{GP}) can be calculated as follows:

$$W_{GP} = \frac{(LAA - AE_{SF})}{(AE_{GP} - AE_{SF})} W_T \quad (1)$$

The mass of each binder was calculated for a reference mass of 5 kg. Table V shows the weight values for PCV, SF and GP for unitary and binary replacements. Using the oxide constituents of each binder determined with XRF (Table IV) the *AE* for the whole mixture was calculated. The total *AE* values are also shown in Table V. As observed, the *AE* of each mixture is inferior to *LAA* (1.5 %).

Table III. Particle size parameters resulting from PSD curves measured using laser light scattering.

raw material	acronym	d_{10} (μm)	d_{50} (μm)	d_{90} (μm)	d_{90}/d_{10}	SSA (cm^2/g)
Portland cement V	PCV	2.2	10.5	30.4	14.7	4209
silica fume	SF	5.1	17.7	36.5	7.2	2468
glass fragments (feed)*	WPG	2800	10000	21100	7.5	n.d.
glass powder [45-75] μm	GP45-75	36.3	56.2	86.9	2.4	499
glass powder [25-45] μm	GP25-45	20.6	39.6	75.6	3.7	692
glass powder < 45 μm	GP45	7.4	20.2	42.0	5.7	1731
glass powder < 25 μm	GP25	4.3	11.9	25.8	6.0	2812

***estimated using manual sieving with five Tyler apertures. n.d: not determined.**

Table IV. Major oxide constituents of the binders measured with XRF spectrometry.

	concentration (%)									LI	AE
binder	SiO_2	CaO	Na_2O	Al_2O_3	MgO	K_2O	Fe_2O_3	SO_3	TiO_2	(%)	(%)
PCV	18.44	60.16	0.18	4.46	5.19	0.89	2.43	4.01	nd	3.79	0.77
SF	92.70	1.03	0.75	0.89	0.68	0.58	0.17	0.16	0.01	3.03	1.13
GP	76.04	11.09	8.04	2.28	0.83	0.59	0.41	0.21	0.06	0.45	8.43

AE: alkaline equivalent (AE = [Na_2O] + 0.658[K_2O]) LI: loss on ignition.

The flow table method was used to estimate the consistency index of the fresh paste according to the ABNT NBR 13276 (2016) standard, which is equivalent to the ASTM C230/C230M-23 (2023) standard. The paste was stored in a truncated-conical apparatus with 125 mm (base) diameter. The spread diameter was measured in X and Y directions after a sequence of 30 rise-and-fall cycles (30 s). The consistency index (CI) was determined as the numeric ratio between the mean diameters resultant from the measurements carried out before and after shaking.

The specimens used for the physical tests were manufactured in accordance with the ABNT NBR 7215 (2019) standard which is equivalent to the ASTM C642 (2021a) standard. The water : binder (PCV+GP+SF) ratio (by weight) was fixed in 0.4 throughout the work. Water and premixed binders were added (in this order) in a 5 L electro-mechanical mixer. The mixing operation was performed in a sequence of three steps, as follows: (i) 1 min mixing at 140 rpm; (ii) 2 min rest; (iii) 2 min mixing at 285 rpm. The paste was transferred into cylindrical molds of 50 x 100 mm. The filled molds were shaken on a low-frequency vibrating table for 5 min. The vibrating time was chosen based on preliminary tests to avoid segregation and exudation effects. The specimens were demolded after 24 h and their dimensions were measured to evaluate the volumetric change. The wet curing was carried out immersing the samples into water. The duration of the wet curing was established according to ABNT NBR 9778 (2005), which is equivalent to ASTM C642 (2021a) standard, as follows: (i) specimens for measurements of water absorption, void index, bulk density, and modulus of elasticity: 28 days (30 samples) (ii) specimens for measurement of compressive strength: 7 days (30 specimens) and 56 days (30 specimens).

Hardened pastes: physical tests, primary phases, microstructure

The tests employed to determine the water absorption, void index and bulk density were performed according to the ABNT NBR 9778 (2005) standard, which is equivalent to the ASTM C642 (2021a) standard. After 28 days of curing, the specimens were weighed to obtain the saturated mass and the mass submerged in water. Afterwards, the specimens were dried in an oven at a temperature of 100 ± 5 ºC for 72 h to determine the dried mass. Water absorption (WA), void index (VI) and the bulk density (ρ), were calculated using standard equations, as follows:

$$WA = \frac{M_S - M_D}{M_D} x100\% \quad (2)$$

$$VI = \frac{M_S - M_D}{M_S - M_{Sb}} x100\% \quad (3)$$

$$\rho = \frac{M_D}{M_S - M_{Sb}} \quad (4)$$

Table V. Mix proportions of pastes with silica fume and glass powder replacements and the values for the alkali equivalent of the whole mixture calculated with XRF data.

		mass (g)			total AE
replacement	**acronym**	**PCV**	**SF**	**GP**	**(%)**
reference	PCV	5000	-	-	0.77
unitary	SF	4750	250	-	0.79
unitary	GP	4750	-	250	1.16
binary	SFGP	4750	237	13	0.81

where M_S, M_D and M_{Sb} are the masses (kg) measured in the saturated, dried, and submersed forms, respectively. $(M_s\text{-}M_{Sb})$ was determined using the Archimedes method. The elastic modulus (E) was determined as a function of the velocity of propagation of the ultrasonic pulse (V) according to ABNT NBR 9778 (2005) and ASTM C597 (2022), as follows:

$$E = \rho . V^2 \frac{(1 + v) .(1 - 2v)}{1 - v} \quad (5)$$

where v is the Poisson coefficient, which is assumed as 0.2 for cements (Kumar-Metha & Monteiro 2014). The sound velocity was measured using Proceq Pundit Lab equipment.

The uniaxial compressive tests (ABNT NBR 7215 2019, ASTM C109M 2021b) were performed using a Shimadzu AGS-X300kN hydraulic press with an imposed loading rate of ~ 0.25 MPa/s. Parallel surfaces on the cylindrical samples were achieved using pairs of elastomeric facers and neoprene discs. The ultimate compressive strength (UCS) was calculated dividing the maximum load by the transversal area of the (unloaded) specimen. Three tests were carried out for each paste for specimens cured during 7 and 56 days. Fragments removed from the core of tested (broken) specimens were collected to perform structural and microstructural characterizations. The fragments were immersed in isopropyl alcohol PA to stop the atmospheric hydration. After 48 h, the fragments (50-100g) were dried in an oven at 50 °C (1 h) and finely crushed (< 75 µm) by hand using a porcelain mortar.

The effect of unitary and binary replacements on the hydration products of PC was assessed using X ray diffraction (XRD) and thermal differential analysis. The XRD patterns were obtained with a Bruker D2-Phaser diffractometer equipped with a Lynxeye one-dimensional detector; Cu-Kα radiation (30 kV, 10 mA; Kα wavelength: 1.54060 Å); goniometer step of 0.0219°/s; counting time 1 s and 2θ scanning from 5° to 80°. The diffracting peaks were indexed using the Bruker AXS Driffrac-Eva software and the COD-2016 data base.

The concentration of hydration products was assessed using thermogravimetry. For this, differential thermal- and thermogravimetric analyses (DTA-TG) were carried out with a Shimadzu DTH 60 equipment. The experiments were carried out from 25 to 1050 °C with a heating rate equal to 12 °C/min in N_2 atmosphere (50 ml/min). Approximately 50 mg of finely crushed powders were tested. The reference material was alumina. The reactions were identified using the recent literature for thermal decomposition of Portland cement (Kabay et al. 2021, Astoveza et al. 2022). The TG diagrams were divided in three parts to assess the weight loss due to water desorption and the thermal decomposition of ettringite (25-250 °C), portlandite (400-550 °C) and calcite (600-850 °C).

The microstructures of pastes aged for 56 days were examined with scanning electron microscopy (SEM) and energy dispersive X ray spectroscopy (EDS). Two fragments of each paste were modeled in resin and dry lapped using sandpaper with decreasing grit sizes from 50 µm (280 mesh) to 5 µm (2500 mesh). The optical polishing was carried out against a rotating (120 rpm) flat disc covered with flocked velvet (FVL) pad using diamond paste with 1 µm grit sizes. The polished surfaces were coated with carbon and SEM images were acquired with a JEOL-JSM-6460 microscope working with secondary (SE) electron beams excited with 30 kV voltage. The X ray emissions of Fe, Ca, K, S, Si, Al, Mg and Na were collected with an Oxford Ultim-Max-40 energy dispersive spectrometer (EDS) coupled to the JEOL microscope. The counting time was set at 3-4 min.

RESULTS AND DISCUSSION

Physical and mechanical properties

Fig. 2 summarizes the values for the consistency index (CI) of the fresh pastes and the void (VI) and water absorption (WA) indexes measured after 28 days of curing. The Fig. 2(a) shows that the particle size of GP affects the CI slightly. Compared to PCV, higher CI values occur for pastes produced with GP < 45 μm and < 25 μm. The addition of SF also enhances the CI. As known, the CI is closely related to the physical characteristics of the fresh paste, which has significant effect on the workability of the cement. Measuring the consistency of pastes modified with GP with d_{50} = 8.4 μm, an increase of more than 10 % was reported for mixed samples in comparison to the control one (Kamali & Ghahremaninezhad 2016). The CI profile shown in Fig. 2(a) agrees with this previous study. These results can be explained by a local increase in the water to cement ratio nearby the surface of large glass particles distributed in cement mixture. Since the workability growth in opposite direction to CI, it is expected that the workability should increase with the GP decreasing, i.e., with the increase in the total specific surface area (SSA) of the replacement material (see Table III).

The effect of the glass particle size on VI and WA is shown in figures 2(b) and 2(c), respectively. The lower values observed for the pastes prepared with finer GP can be explained considering the amount of water trapped at the PC-GP particle interfaces (the so-called kneading water) during maturation. Coarse particles with relatively smaller SSA contribute to an increase in the amount of kneading water, i.e., a higher amount of water can be trapped in coarse particle interstices. During drying at 100 °C, the kneading water evaporates giving rise to a high concentration of pores and, consequently, higher values for VI and WA indexes are found. From Table III, it is observed that the SSA of SF and fine GP fractions (< 45 and < 25 μm) are approximately 2 times smaller compared to PCV whereas this difference reaches approximately 6 and 8 times for [25-45] μm and [45-75] μm fractions, respectively. The results in Fig. 2 also show that the role played by SF on VI and WA indexes in binary mixtures is less important than that observed on CI. Thus, based on VI and WA examinations, it is possible to suggest that the unitary replacement with GP < 45 μm is a suitable choice for PC substitution.

A similar effect as that shown in Fig. 2 for CI was observed in a study using higher percentages of GP and broad ranges for GP particle size (Afshinnia & Rangaraju 2015). These authors reported that

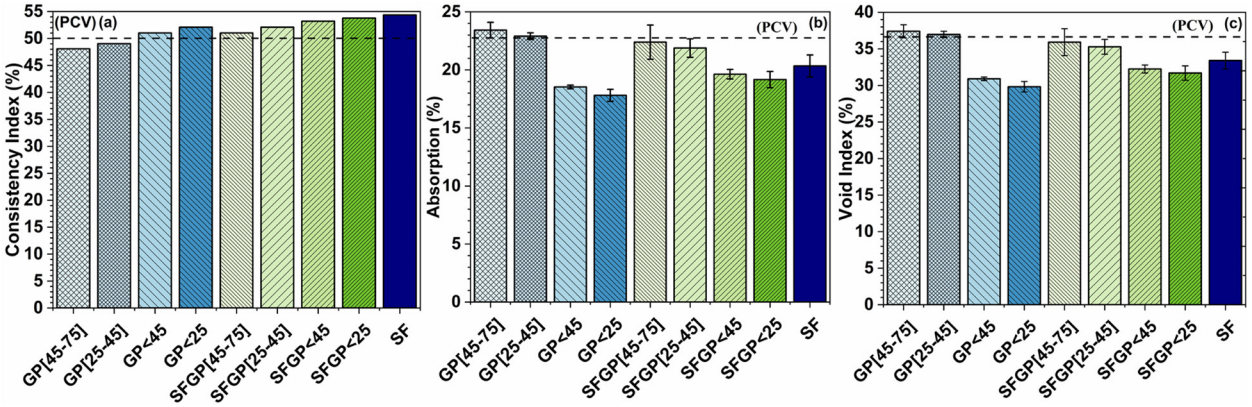

Figure 2. Consistency index (a) of pastes casted with GP and/or SF replacements for PCV cement and the respective void (b) and water absorption (c) indexes measured after 28 days of curing. Error bars are 1σ calculated for 3 tests.

mortars produced with GP with d_{50} = 70 μm (d_{90}/d_{10} ≈ 14) using replacement dosages varying between 5 wt% and 20 wt% had higher workability than the respective replacement dosages with d_{50} = 17 μm (d_{90}/d_{10} ≈ 45). In another study, Afshinnia & Rangaraju (2016) observed that the air content increased approximately 50 % when 20 wt% of GP with d_{50} = 17 μm was used for concrete casting. The large heterogeneity in PSD of glass powder may explain the significant number of voids in their samples. For the same water:cement ratio, a higher water absorption may contribute to a higher concentration of voids after curing. The higher reactivity expected for fine GP and SF particles can result in higher amounts of hydrated products and, consequently, lower values for VI. The results in Fig. 2 suggest that low rates of GP < 45 μm are enough to cause a decrease in WA and VI keeping a satisfactory workability compared to the reference sample.

In Fig. 3, it is shown the values of ρ and E measured for the pastes cast with GP and SF substitutions. The bulk density values shown in Fig. 3(a) are practically identical. A weak effect of GP in ρ (~ 2-3% inferior to the control sample) of concrete mixtures prepared with 20 wt% of replacement was previously observed (Afshinnia & Rangaraju 2016). Compared to the reference sample, a slight reduction in E is observed for the pastes mixed with GP [45-75] μm and a slight increase in E occurred for replacements with GP < 45 μm and GP < 25 μm. These results suggest that a higher concentration of voids found in samples prepared with coarse GP is probably attenuating the propagation of elastic waves and, according to Eq. [2], a decrease in stiffness is occurring since ρ remains unchanged. The E values measured for the specimens prepared with SF substitutions are practically the same as that found for the reference sample. Compared to GP substitutions, the replacement with SF caused a slight reduction in E.

The UCS measured after 7 and 56 days are shown in Fig. 4. A similar trend is noticed for both ages of testing. Only the cement pastes prepared with unitary replacements using [45-75] μm and [25-45] μm particles had the mean values lower than the value found for the reference sample. At 56 days, it is observed that UCS for the pastes prepared with < 45 μm and < 25 μm (unitary) replacements increased, on average, by 4 % and 7 %, compared to PCV. This is a promising result since the amount of replacement used in this study is much lower compared to previous works. As noted, numerous investigations studied the effect of glass particle size on the compressive strength of concretes using replacement dosages between 10 and 30 wt% (Shao et al. 2000, Özkan & Yüskel 2008, Afshinnia & Rangaraju 2015). At 56 days, binary replacements with GP particles < 45 μm and < 25 μm caused an average UCS increase of 12 % and 21 % in comparison to PCV. The binary replacement with GP < 25 μm offered the best mechanical performance, which suggests that low dosage of fine GP in association with SF can still enhance the compressive strength of cement pastes. The importance of the GP particle size is confirmed by comparing the UCS values for [45-75] μm and < 25 μm in Fig. 4(b): a 20% difference in UCS mean values was observed for a replacement dosage as low as 5 wt%. According to Afshinnia & Rangaraju (2016), particle size and curing age are the main factors affecting the mechanical strength of concrete containing GP as ASCM. The age effect on UCS shown in Fig. 4 follows the regular trend observed in previous studies. It will be discussed in *Property correlation and microstructure*.

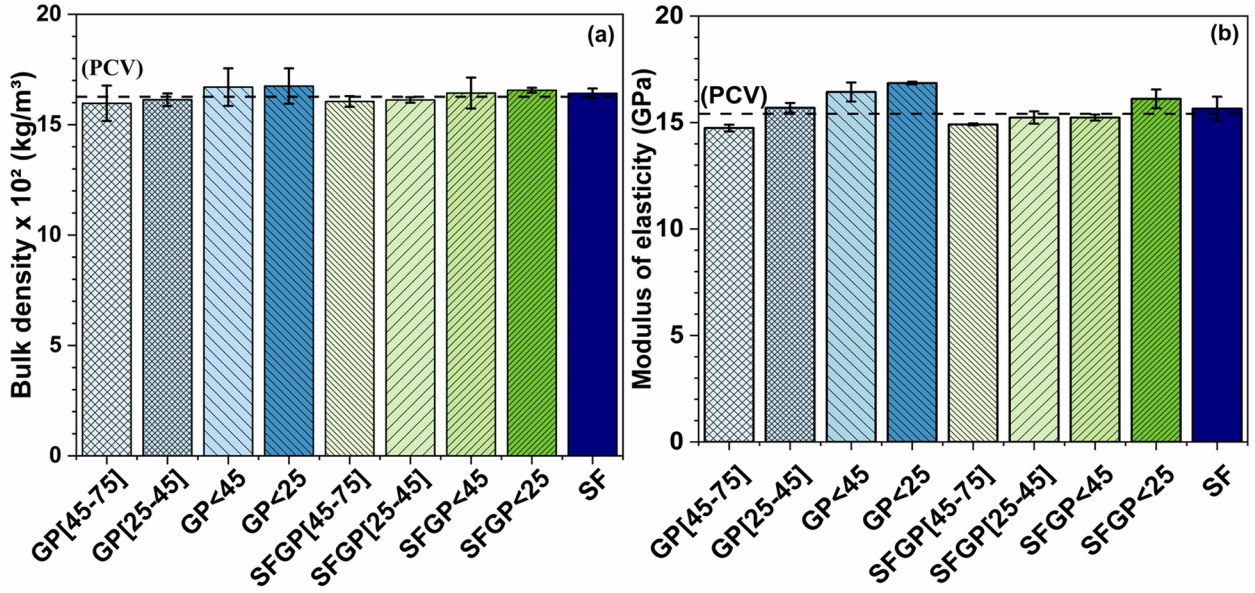

Figure 3. Bulk density (a) and elastic modulus (b) of pastes cast with GP and/or SF replacements for PCV cement measured after 28 days curing. Error bars are 1σ calculated for 3 tests.

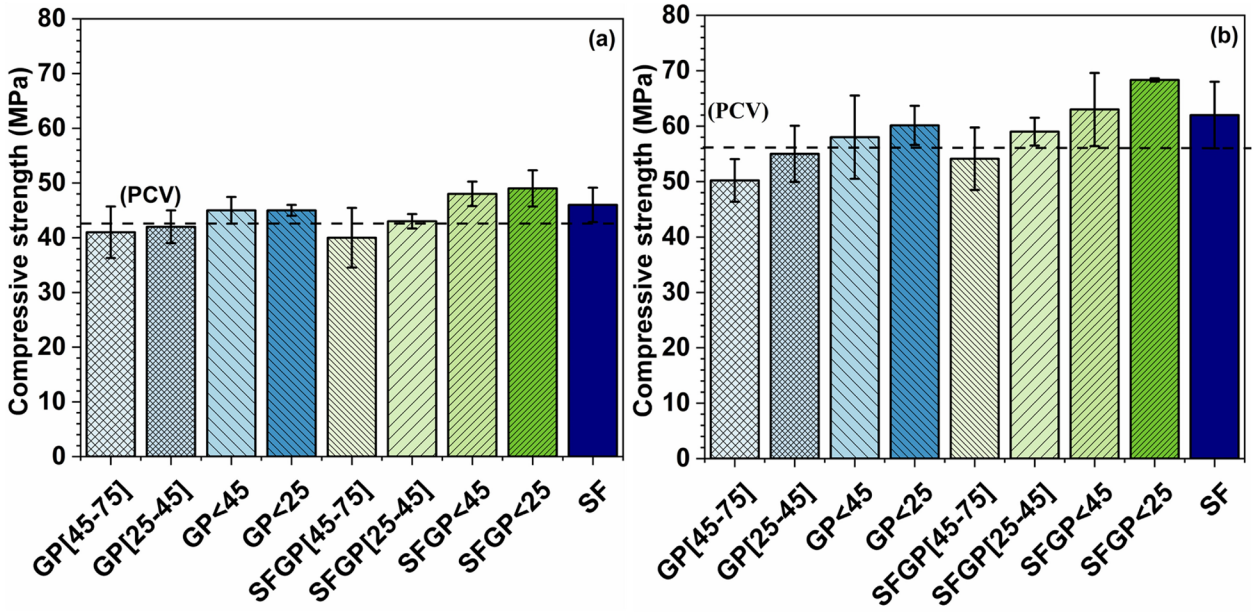

Figure 4. Ultimate compressive strength of pastes prepared with GP and/or SF replacements for PCV cement measured after 7 days (a) and 56 days (b) of curing. Error bars are 1σ calculated for 3 tests.

Hydration products

Typical XRD patterns of cementitious pastes prepared with GP and SF replacements are shown in Fig. 5. No significant differences were observed in peak positions in comparison with typical hydration phases reported in the recent literature (Du & Tan 2017, Kabay et al. 2021, Ruan et al. 2022). The major constituents found in our samples were ettringite ($3CaO.Al_2O_3.3CaSO_4.32H_2O$), portlandite ($Ca(OH)_2$) and C-S-H (calcium-silicate-hydrates). Periclase (MgO), calcite and dolomite are mineral phases currently found in PC. As known, the peak intensities in powder diffractograms are affected by experimental

aspects such as the intensity of the primary X ray beam, the instrumental optics and the preferential orientation of crystalline grains resulting from sample preparation (Hubbard & Snyder 1988, De Matos et al. 2022). Thus, no reliable information owing to concentration of constituent phases can be drawn from a direct calculation of peak heights and the integrated intensities. The assessment of the concentration of cementitious phases using the so-called Rietveld refinement method (Rietveld 2014, van Laar & Schenk 2017) is being performed and will be discussed in a future article. Thus, the main outcome of the XRD analysis carried out so far is the certification that the low dosages of SF and GP in different particle size ranges did not affect the hydration phases of the cement pastes.

From the qualitative point of view, the same thermal reactions were observed after 7 and 56 days. As observed in DTA diagrams shown in Fig. 6(a), the replacement of PCV for GP and SF did not affect the thermal decompositions of the ettringite, portlandite, C-S-H and calcite. As previously observed (Jawed & Skalny 1978, Du & Tan 2014), the thermal decomposition of portlandite was observed at approximately 480 °C. The shift in calcite decomposition towards slightly higher temperature

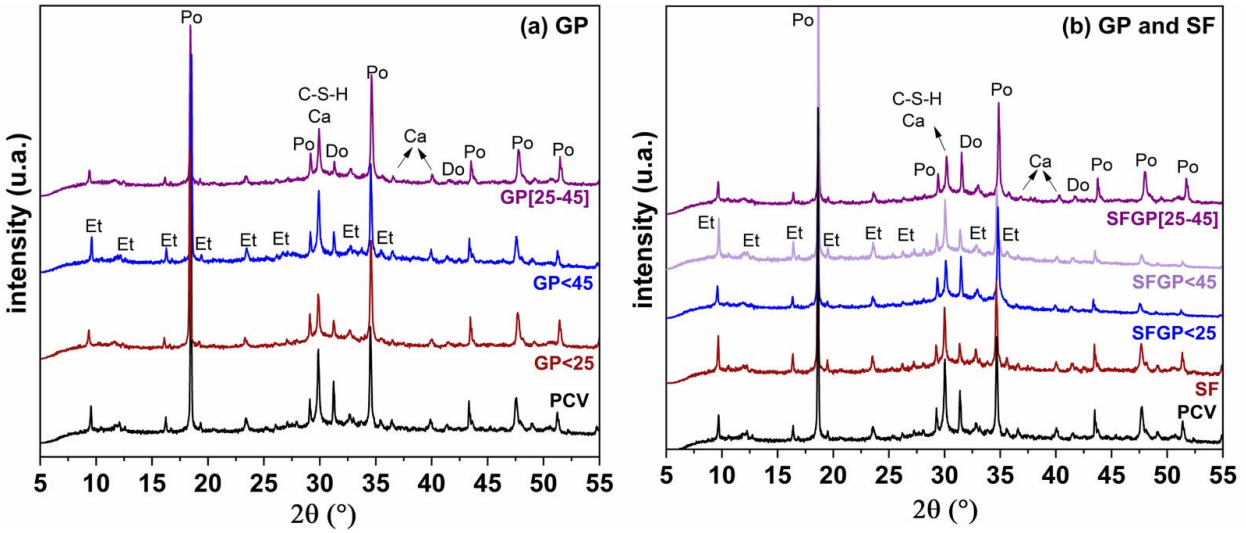

Figure 5. XRD patterns of PCV pastes with unitary (a) and binary (b) GP and SF replacements obtained after 56 days of curing. Ca: Calcite; C-S-H: Calcium-Silicate-Hydrates; Do: Dolomite; Et: Ettringite; Po: Portlandite.

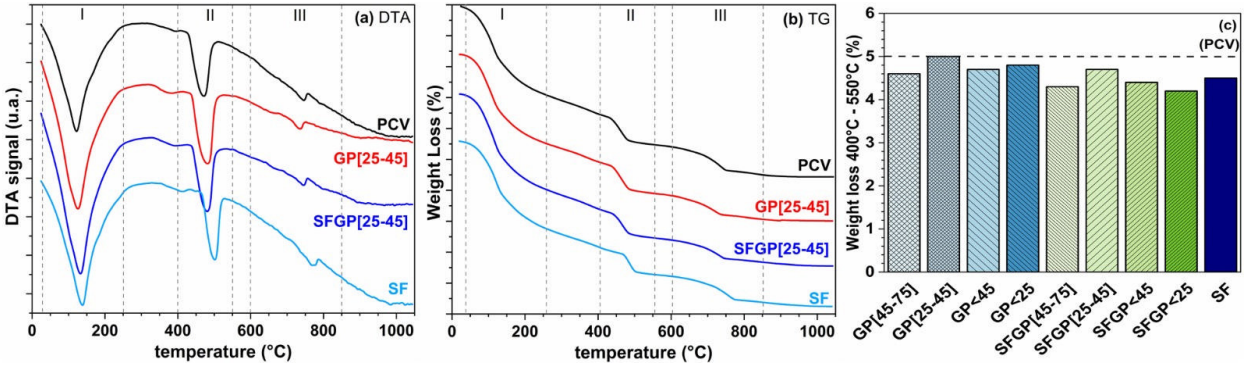

Figure 6. DTA (a) and TG (b) diagrams of PCV, SF, GP[25-45] and SFGP[25-45] pastes after 56 days of curing. Dotted lines define the thermal decomposition regions used to calculate the weight loss for ettringite (I), portlandite (II) and calcite (III). The weight loss related to portlandite decomposition (region II) for all samples is shown in (c).

observed in samples prepared with SF substitution (760 °C) did not affect the physical properties of the hardened pastes.

Typical TG diagrams related to the whole decomposition are shown in Fig. 6(b). Besides water desorption, the region between 25 and 250 °C (region I) is related to the decomposition of ettringite and the beginning of C-S-H decomposition. In this region, the weight loss remained practically unchanged around 14.5 % for all pastes. The decomposition of portlandite stated in region II (400-550 °C) was affected for both unitary and binary substitutions. This effect is better observed in Fig. 6(c) where a noticeable weight loss decrease was observed for all replacements in comparison to the reference except for the unitary [25-45] μm replacement. For this sample, the test was repeated twice, obtaining a dispersion better than 2 %. For the region III, the weight loss due to calcite decomposition remained almost unchanged varying between 4.8 and 5.0 % for all samples.

The concentrations of portlandite for 7-day and 56-day hardened pastes are shown in Fig. 7. This concentration was calculated using the relationship between the weight loss measured between 400° C to 550° C due to portlandite decomposition and the ratio between the atomic weights of H_2O and $Ca(OH)_2$. The concentration found for the reference sample after 56 days (20.6 %) is similar to values reported in literature for curing periods between 28 and 91 days (Du & Tan 2014). For mixed pastes, the concentrations after 7 days suggests that GP inhibits the portlandite consumption during the early period of curing, i.e., the hydration reactions in mixed pastes occurred at lower rates compared to the reference sample. On the contrary, Fig. 7(b) indicates that the portlandite consumption after 56 days is higher for mixed pastes in comparison with the reference sample. It is also observed that the particle size of GP has an important role for prolonged curing time. In the present stage of this study, the higher consumption of portlandite for SFGP pastes can be explained considering the effects of the kneading water associated with GP surfaces and the increase in pozzolanic reactivity due to SF and GP. As known, the kneading water impact on the hydration of the cement-silica system for

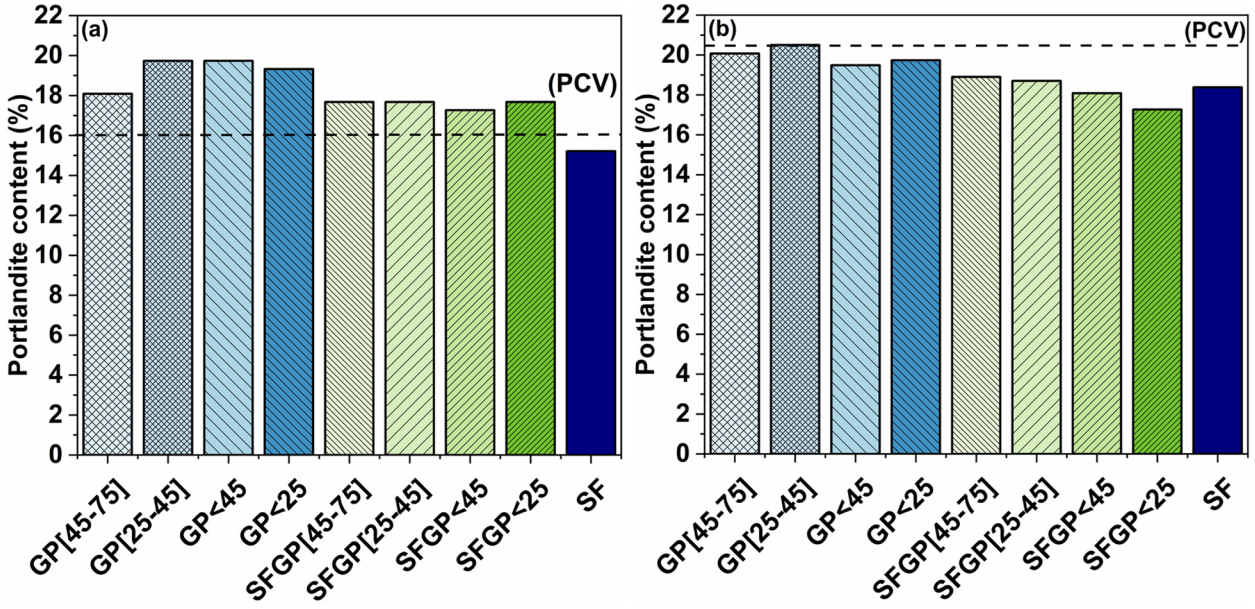

Figure 7. Portlandite concentrations calculated from TG analysis carried out in hardened pastes prepared with low dosage of GP and SF replacements after 7 days (a) and 56 days (b) of curing. The experimental scattering is estimated better than 2 %.

prolonged periods of curing, which contributes to the consumption of portlandite. In turn, the higher dissolution expected for GP < 45 μm and GP < 25 μm particles becomes the cement medium more alkaline contributing to the increase of the pozzolanic reactivity of the pastes prepared with binary substitutions.

The significance of GP replacement on portlandite consumption reported in previous studies was higher compared to the quantities shown in Fig. 7. Investigating the effect of the amount of substitution of PC for GP with a median particle size of 10 μm, Du & Tan (2014) concluded that the concentration of portlandite decreased by ~ 12 % for pastes prepared with 30 wt% of GP after a curing age of 91 days. They also found that portlandite was almost depleted after 91 days when 60 wt% of cement was replaced by GP. Moreover, investigating the role of chemical composition of GP during the hardening process of mortar samples prepared with 25 wt% cement replacement, Bignozzi et al. (2015) determined a portlandite consumption higher than 7 % for mixed samples in comparison with the reference sample for a curing age of 60 days. However, the studies using high dosage of GP replacement did not consider the harmful effect of alkali-silica reaction (ASR) over long term periods. As known, the absence of volumetric expansion is not sufficient to prove the non-existence of ASR microscopically (Shao et al. 2000, Idir et al. 2011, Du & Tan 2017). Thus, the results of the present study demonstrating the possibility to gain some increase in portlandite consumption in pastes prepared with low substitution rates of GP with particle size < 45 μm is a feasible issue from the practical point of view.

Property correlation and microstructure

The consumption of portlandite was the main indicator of the pozzolanic reactivity assessed in the present study. Thus, an attempt to correlate this parameter with physical properties is shown in Fig. 8. The void index (VI) was chosen since it reflects the existence of volumetric defects (porosities

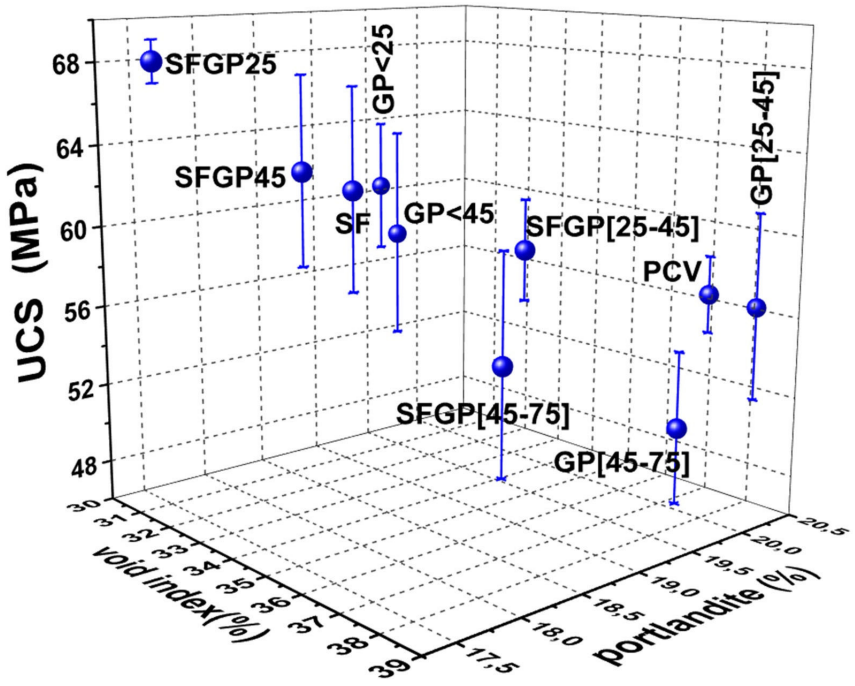

Figure 8. Relationship between the void index and the portlandite concentration with the compressive strength (UCS) of cementitious pastes prepared with GP and SF substitutions. Error bar corresponds to 1σ calculated for 3 tests carried out after 56 days of curing.

and cracks) that play, among other things, a crucial role on the mechanical strength of cementitious materials (Metha & Ashish 2020, Boukhelf et al. 2021). Additionally, a VI decreasing by ~ 6 % measured for GP < 45 μm and < 25 μm substitutions (Fig. 2(b)) is a suitable indicator to support the adoption of low substitution rates of fine GP in mortar and concrete production. Previously, Kamali & Ghahremaninezhad (2016) observed a reduction of ~ 3 % in pore volume for pastes prepared with 20 wt% of GP substitution (d_{50} = 8.4 μm) after 28 days of curing. Although the dispersion related to UCS values is large due to the small number of tests, the 3D plot in Fig. 8 shows a fair dependence of UCS with the decrease of VI and the remaining content of portlandite. Compared to reference (PCV), the pastes prepared with fine GP substitutions indicate that the incorporation of low dosage of glass particles < 45 μm has a favorable contribution to reduce the void index and to increase the pozzolanic reactivity. As noted, the unitary and binary pastes prepared with GP[45-75] deviate from the whole behavior in relation the portlandite consumption. These pastes show lower portlandite content compared to the values measured for PCV that showed slightly higher value for UCS. Even though, the positive effect of GP < 45 μm and GP < 25 μm on VI and portlandite content are reflecting on UCS values. To further examine this result, an overview of the microstructure and the elemental distribution observed in some pastes are shown in Fig. 9.

SEM and EDS images shown in Fig. 9 summarize the microscopic features resultant from GP and SF incorporation into cementitious pastes after 56 days of curing. Coarse particles of glass were much easier to be observed in the cement matrix than fines independent from the magnification adopted. Cracks were randomly observed and, at least roughly, no correlation was observed between crack extension and glass particle size. In several cases, as those documented in figures 9(a) and 9(d), the crack path deviates from coarse glass particles. This feature suggests that GP is playing the role of hardened particles merged into a brittle matrix. The edge shape of glass particles resultant from dry grinding is more evident in figures 9(a) and 9(d) than in Fig. 9(b). Probably, the irregular faces of glass particles observed in Fig 9(b) is a consequence of higher dissolution rates occurring in fine glass fragments. The high pozzolanic reactivity of ground glass particles < 50 um was previously highlighted in mortar mix prepared high replacement rate (> 20 wt%) of GP (Shi et al. 2005, Idir et al. 2011). Figures 9(b) and 9(c) show, respectively, SE image and EDS signal of the GP<45 paste. These figures spatially correlate the variation in GP shape and the change in Ca and Si signal intensities, which reinforces the assumption that the consumption of silica during the pozzolanic reaction has a close dependence with glass particle size. The partial GP dissolution noticed Fig. 9(b) may explain at least in part the difficult in identifying glass traces, similar as that shown in Fig. 9(h), in pastes prepared with GP < 25 μm. As noticed in figures 9(d) and 9(g), SF used in this study usually occurs as round agglomerates with several tens micrometers. Crack propagation throughout SF agglomerates as that registered in Fig. 9(g) was frequently observed. These features suggest that the poor stabilization of individual SF particles into the cement matrix affects the pozzolanic reactivity as Fig. 8 suggests.

Na and Mg signal maps as those shown in figures 9(f) and 9(i) were important to identity individual particles of glass and dolomite, respectively. Dolomite with few micrometers' length were observed in all samples, which confirms that it is originated from raw materials used during the clinker production. Na records were also important to distinguish Si-rich concentrations originated from glass particle (high Na signal intensity) and hydration products such as C-S-H. For instance, the distribution of Si and Ca signals pertaining to the circular region underlined in Fig. 9(e) suggests a

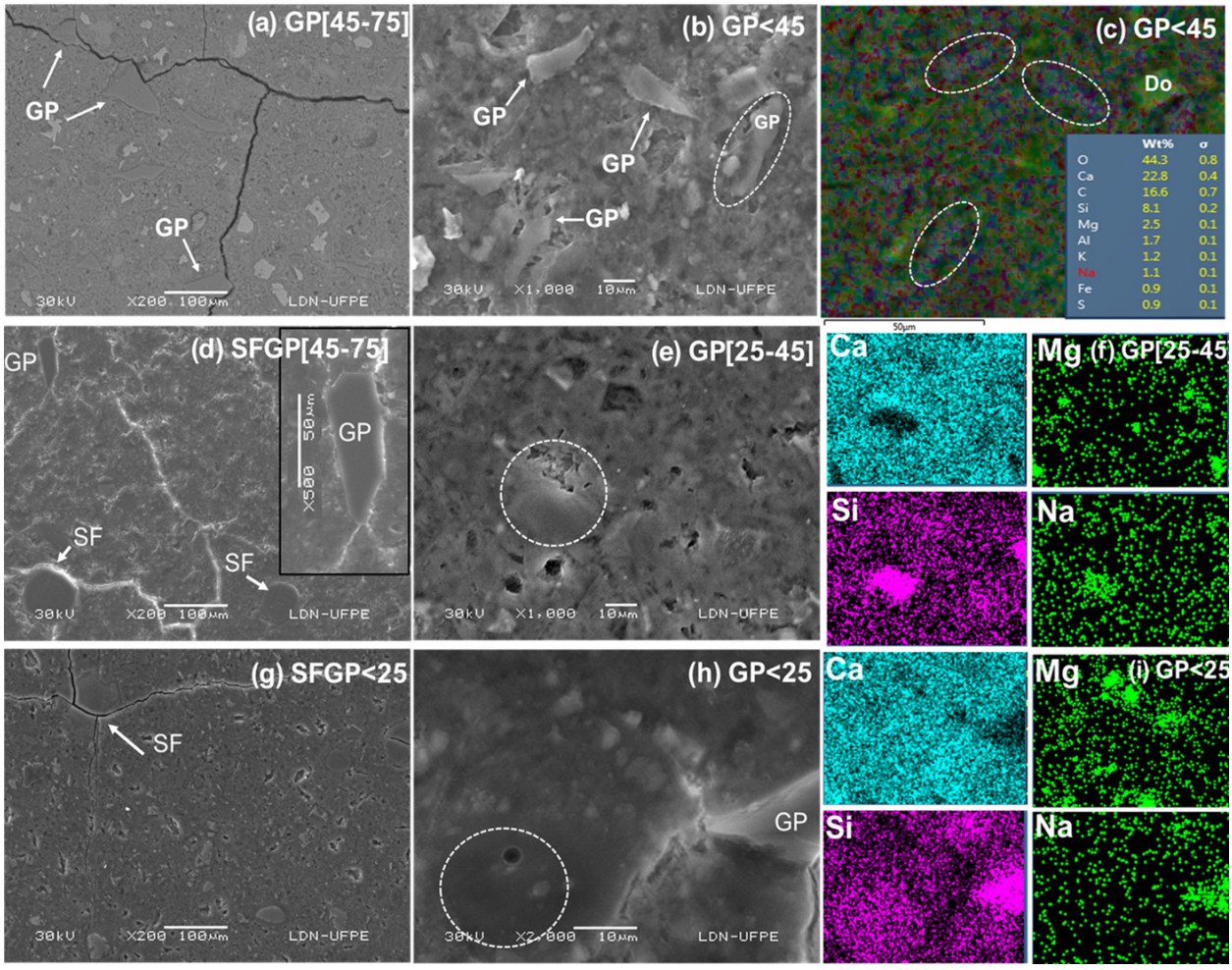

Figure 9. Secondary-electrons SEM images (a, b, d, e, g, h) and EDS signal distributions of Ca, Mg, Si and Na elements (c, f, i) observed in PCV pastes prepared with low dosage replacements of [45-75] µm, [25-45] µm, < 45 µm and < 25 µm glass powder (GP) and silica fume (SF) after 56 days of curing. EDS maps shown in (c), (f) and (i) are spatially related to (b), (e) and (h) SE images, respectively. Dark green and purple colors in (c) denote Ca-rich and Si-rich regions, respectively.

spatial relationship between silica derived from an undissolved glass particle and portlandite. As noticed, the intensity of Ca signal is higher in the upper part of the circular region where Si signal is deficient. Now, observing the circular region labeled in Fig. 9(h) and the respective region in EDS map in Fig. 9(g), it is concluded that the distribution of Si and Ca are more uniform, which suggests that the consumption of portlandite rises the formation of C-S-H. This behavior is opposite as that observed in the left side of Fig. 9(i) where the intensities for Si and Na signals suggest lower dissolution rates for GP particles and, consequently, less significant formation of C-S-H.

CONCLUSION

This study investigated the particle size effect of glass on physical and microstructural properties of cement pastes prepared with silica fume and low dosage replacements of waste packing glass

recycled in the Brazilian Northeastern. Unitary and binary substitutions were stated to achieve an alkaline equivalent limit < 1.5 wt%. The findings of this study can be summarized as follows:

(i) the void index and the ultimate compressive strength of hardened pastes aged for 56 days were positively affected when glass particles < 45 μm replaced 5 wt% of the Portland cement. A similar trend was observed for binary substitutions. Consistency index, bulk density, and the modulus of elasticity remained practically unchanged due to the low replacement rate employed.

(ii) the disappearing of the edge-shaped morphology of as-ground glass particles < 45 μm observed in hardened pastes was the main microscopic indication for the pozzolanic reactivity of waste glass powder used in this study. This result confirmed the trend observed for portlandite consumption assessed with thermogravimetry. Large size agglomerates of silica fume observed in hardened pastes revealed the importance to improve the surface stability of ultrafine particles of this pozzolan prior to mixing.

(iii) the compressive strength of hardened pastes aged for 56 days was simultaneously affected by void index and portlandite consumption. This result led to the conclusion that, among the mixtures investigated, glass powder with particle size < 45 μm seems to be a satisfactory conciliation between the improvement in the physical properties of cement pastes and the time required for glass cullet processing.

Acknowledgments

The authors were grateful to *CSN Alhandra – Cimento Elizabeth* (Alhandra, PB) for the Portland cement samples and the X ray fluorescence analysis. They were also grateful to *Fausto Soluções Ambientais Ltda,* (Recife, PE) for supplying them with waste packing glass. The grinding and screening operations were carried out with the assistance of Technician Marcelo F. Gomes (LTM, Department of Mining Engineering). The authors are grateful to Pró-Reitoria de Pesquisa e Inovação of the Universidade Federal de Pernambuco (UFPE P: 23076.074512/2020-23) and Conselho Nacional de Desenvolvimento Científico e Tecnológico (CNPq P:420002/2016-2; CNPq P: 310635/2021-07) for the financial support to this research. FBMB is grateful to Fundação de Amparo à Ciência e Tecnologia de Pernambuco (FACEPE IBPG-0057-3.01/21) for the scholarship provided. The authors dedicate this study to the *Carroceiros* of Brazil.

REFERENCES

ABNT - ASSOCIAÇÃO BRASILEIRA DE NORMAS TÉCNICAS. 2005. NBR 9778: Argamassa e concreto endurecidos - Determinação da absorção de água, índice de vazios e massa específica. Rio de Janeiro (in Portuguese).

ABNT - ASSOCIAÇÃO BRASILEIRA DE NORMAS TÉCNICAS. 2016. NBR 13276: Argamassa para assentamento e revestimento de paredes e tetos - Determinação do índice de consistência. Rio de Janeiro (in Portuguese).

ABNT - ASSOCIAÇÃO BRASILEIRA DE NORMAS TÉCNICAS. 2018. NBR 16697: Cimento Portland - Requisitos. Rio de Janeiro (in Portuguese).

ABNT - ASSOCIAÇÃO BRASILEIRA DE NORMAS TÉCNICAS. 2019. NBR 7215: Cimento Portland - Determinação da resistência à compressão de corpos de prova cilíndricos. Rio de Janeiro (in Portuguese).

AFSHINNIA K & RANGARAJU PR. 2015. Influence of fineness of ground recycled glass on mitigation of alkali-silica reaction in mortars. Constr Build Mater 81: 257-267.

AFSHINNIA K & RANGARAJU PR. 2016. Impact of combined use of ground glass powder and crushed glass aggregate on selected properties of Portland cement concrete. Constr Build Mater 117: 263-272.

ALI MB, SAIDUR R & HOUSSAIN MS. 2011. A review on emission in cement industries. Renew Sustain Ener Rev 15: 2252-2261.

ALVARENGA CBCS, HEIDERICK OM, COUTO TA, CETLIN PR, SALES RBC & AGUILAR MTP. 2019. Influence of soda-lime waste glass microparticles on workability and thermal properties of Portland cement compounds. Mat Construction 69(335): 1-9.

ASTM - AMERICAN SOCIETY FOR TESTING AND MATERIALS. 2020. C1778. Reducing the Risk of Deleterious Alkali-Aggregate Reaction in Concrete. West Conshohocken, PA.

ASTM - AMERICAN SOCIETY FOR TESTING AND MATERIALS. 2021a. C642. Standard test method for density, absorption, and voids in hardened concrete. West Conshohocken, PA.

ASTM - AMERICAN SOCIETY FOR TESTING AND MATERIALS. 2021b. C109M. Standard test method for compressive strength of hydraulic cement mortars. West Conshohocken, PA.

ASTM - AMERICAN SOCIETY FOR TESTING AND MATERIALS. 2022. C597. Standard test method for pulse velocity through concrete. West Conshohocken, PA.

ASTM - AMERICAN SOCIETY FOR TESTING MATERIALS. 2023. C230/C230M-23. Standard specification for flow table for use in tests of hydraulic cement. West Conshohocken, PA.

ASTOVEZA J, TRAUCHESSEC R, MIGOT-CHOUX S, SOTH R & PONTIKES Y. 2022. Iron-rich slag addition in ternary binders of Portland cement, aluminate cement and calcium sulfate. Cem Concr Res 153: 106689.

AUSTIN LG & BAGGA P. 1981. An analysis of fine dry grinding in ball mills. Powder Technol 28: 83-90.

BIGNOZZI MC, SACCANI A, BARBIERI L & LANCELLOTTI I. 2015. Glass waste as supplementary cementing materials: The effects of glass chemical composition. Cement Concr Compos 55: 45-52.

BOUKHELF F, CHERIF R, TRABELSI A, BELARBI R & BOUIAFJARA MB. 2021. On the hydrothermal behavior of concrete containing glass powder and silica fume. J Clean Product 318: 12847.

CARSANA M, FRASSONI M & BERTOLINI L. 2014. Comparison of ground waste glass with other supplementary cementitious materials. Cement Concr Compos 45: 39-45.

DE MATOS PR, ANDRADE NETO JS, JANSEN D, DE LA TORRE AG, KIRCHHEIN AP, CAMPOS CEM. 2022. In-situ laboratory X-ray diffraction applied to assess cement hydration. Cem Concr Res 162: 106988.

DU H & TAN KH. 2014. Waste glass powder as cement replacement in concrete. J Adv Concr Technol 12: 468-477.

DU H & TAN KH. 2017. Properties of high-volume glass powder concrete. Cement Concr Compos 75: 22-29.

FEDERICO LM & CHIDIAC SE. 2009. Waste glass as a supplementary cementitious material in concrete – Critical review of treatment methods. Cement Concr Compos 31: 606-610.

FUERSTENAU DW & ABOUZEID AZM. 2002. The energy efficiency of ball milling in comminution. Intl J Miner Process 67: 161-185.

GCCA - GLOBAL CEMENT AND CONCRETE ASSOCIATION. 2020. Total gross CO_2 emissions excluding CO_2 from power generation grey white cement. 2020. https://gccassociation.org/gnr/world/GNR-Indicator_59cTGW-world.html. March. 1st 2021.

GUZZO PL, MARINHO DE BARROS FB, SOARES BR & SANTOS JB. 2020. Evaluation of particle size reduction and agglomeration in dry grinding of natural quartz in a planetary ball mill. Powder Technol 368: 149-159.

HUBBARD CR & SNYDER RL. 1988. RIR – Measurement and use in quantitative XRD. Powder Diffract 3(2): 74-77.

IDIR R, CYR M & TAGNIT-HAMOU A. 2011. Pozzolanic properties of fine and coarse color-mixed glass cullet. Cement Concr Compos 33: 19-29.

ISMAIL ZZ & AL-HASHMI EA. 2009. Recycling of waste glass as a partial replacement for fine aggregate in concrete. Waste Manag 29: 655-659.

JANI Y & HOGLAND W. 2014. Waste glass in the production of cement and concrete – A review. J Environ Chem Eng 2: 1767-1775.

JAWED I & SKALNY J. 1978. Alkalis in cement: a review II. Effects of alkalis on hydration and performance of Portland cement. Cem Concr Res 8(1978): 37-51.

KABAY N, MIYAN N & ÖZHAN H. 2021. Utilization of pumice powder and glass microspheres in cement mortar using paste replacement methodology. Constr Build Mater 282: 122691.

KAMALI M & GHAHREMANINEZHAD A. 2016. An investigation into the hydration and microstructure of cement pastes modified with glass powders. Constr Build Mater 112: 915-924.

KHRIMI A, CHAABOUNI M & SAMET B. 2013. Chemical behaviour of ground waste glass when used as partial waste glass in cements. Constr Build Mater 44: 74-80.

KUMAR-MEHTA P & MONTEIRO PJM. 2014. Concreto: Microestrutura, Propriedades e Materiais. Editor: N. P. Hasparyk,2nd ed, IBRACON, São Paulo, p. 175. (in Portuguese).

LOTHENBACH B, SCRIVENER K & HOOTON RD. 2011. Supplementary cementitious materials. Cem Concr Res 41: 1244-1256.

MATOS AM & COUTINHO JS. 2012. The durability of mortar using waste glass powder as cement replacement. Constr Build Mater 26: 205-215.

METHA A & ASHISH DK. 2020. Silica fume and waste glass in cement concrete production: a review. J Build Eng 29: 100888.

MMA/SNIR - MINISTÉRIO DO MEIO AMBIENTE/SISTEMA NACIONAL DE INFORMAÇÕES SOBRE A GESTÃO DOS RESÍDUOS SÓLIDOS. 2020. Relatório Nacional de Gestão de Resíduos Sólidos. Available in: https://sinir.gov.br/relatorios/nacional/. Download in Sep. 10th 2020 (in Portuguese).

MOHAJERANI A, VAJNA J, CHEUNG HH, KURMUS H, ARULRAJAH A & HORPIBULSUK S. 2017. Practical recycling applications of crushed waste glass in construction materials: A review. Constr Build Mater 156: 443-467.

OLIVEIRA SA, RIBEIRO ARB & SOBRAL MFF. 2022. A perspectiva de catadores de materiais recicláveis sobre seu trabalho: incentivos e desafios em uma cidade de um país em desenvolvimento. Rev Gest Soc Amb 16: 1-17. (in Portuguese).

OMRAN AF, D-MORIAN E, HARBEC D & TAGNIT-HAMOU A. 2017. Long-term performance of glass-powder concrete in large-scale field applications. Constr Build Mater 135: 43-58.

ÖZKAN Ö & YŰSKEL I. 2008. Studies on mortars containing waste bottle glass and industrial by-products. Constr Build Mater 22: 1288-1298.

PARK SB, LEE BC & KIM JH. 2004. Studies on mechanical properties of concrete containing waste glass aggregate. Cem Concr Res 34: 2181-2189.

RIETVELD HM. 2014. The Rietveld method. Phys Scripta 89(9): 098002.

RUAN Y, JAMIL T, HU C, GAUTAM BP & YU J. 2022. Microstructure and mechanical properties of sustainable cementitious materials with ultra-high substitution level of calcined clay and limestone. Constr Build Mater 314: 125416.

SHAO Y, LEFORT T, MORAS S & RODRIGUEZ D. 2000. Studies on concrete containing ground waste glass, Cem Concr Res 30: 91-100.

SHI C, WU Y, RIEFLER C & WANG H. 2005. Characteristics and pozzolanic reactivity of glass powders. Cem Concr Res 35: 987-993.

SINGH LP, GOEL A, BHATTACHARYYA SK & MISHRA G. 2016. Quantification of hydration products in cementitious materials incorporating silica nanoparticles. Frontiers Struc Civil Eng 10: 162-167.

SOARES BR & GUZZO PL. 2019. Moagem ultrafina de quartzo natural em moinhos de alta energia: um estudo comparativo. XXVIII Encontro Nacional de Tratamentos de Minérios e Metalurgia Extrativa (ENTMME 2019), Belo Horizonte, Brasil, p. 1-8.

SURANENI P & WEISS J. 2017. Examining the pozzolanicity of supplementary cementitious materials using isothermal calorimetry and thermogravimetric analysis. Cement Concr Compos 83: 273-278.

VAITKEVIČIUS V, ERELIS E & HILBIG H. 2014. The effect of glass powder on the microstructure of ultrahigh performance concrete. Constr Build Mater 68: 102-109.

VAN LAAR B & SCHENK H. 2017. The development of powder profile refinement at the Reactor Centre Netherlands at Petten. Acta Crystallogr A74: 88-92.

YOU I, YOO DY, DOH JH & ZI G. 2021. Performance of glass-blended cement produced by intergrinding and separate grinding methods. Cement Concr Compos 118: 103937.

ZHANG Q, KANO J & SAITO F. 2007. Fine grinding of materials in dry systems and mechanochemistry. In: Salman AD, Ghadini M & Hounslow MJ (Eds), Handbook Powder Technol 12: 509-528.

ZHENG K. 2016. Pozzolanic reaction of glass powder and its role in controlling alkali-silica reaction. Cement Concr Compos 67: 30-38.

How to cite

PATRIOTA ALS, BARROS FBM, CARNEIRO AMP & GUZZO PL. 2024. An investigation on the physical properties of cementitious pastes modified with low dosage of waste glass powder and silica fume. An Acad Bras Cienc 96: e20231153. DOI 10.1590/0001-3765202420231153.

Manuscript received on October 15, 2023;
accepted form publication on April 12, 2024

ANDRÉ L.S. PATRIOTA[1,2]
https://orcid.org/0000-0002-3179-1867

FILIPE B.M. BARROS[2,4]
https://orcid.org/0000-0002-5447-7213

ARNALDO M.P. CARNEIRO[2,3]
https://orcid.org/0000-0002-4279-7156

PEDRO L. GUZZO[4]
https://orcid.org/0000-0003-3415-8618

[1]Instituto Federal de Educação, Ciência e Tecnologia do Sertão Pernambucano, Departamento de Construção Civil, Campus Salgueiro, BR-232, Km 508, s/n, Zona Rural, 56000-000 Salgueiro, PE, Brazil

[2]Programa de Pós-Graduação em Engenharia Civil, Universidade Federal de Pernambuco, Avenida da Arquitetura, s/n, Cidade Universitária, 50740-550 Recife, PE, Brazil

[3]Universidade Federal de Pernambuco, Departamento de Engenharia Civil, Avenida da Arquitetura, s/n, Cidade Universitária, 50740-550 Recife, PE, Brazil

[4]Universidade Federal de Pernambuco, Departamento de Engenharia de Minas, Avenida da Arquitetura, s/n, Cidade Universitária, 50740-550 Recife, PE, Brazil

Correspondence to: **Pedro Luiz Guzzo**
E-mail: pedro.guzzo@ufpe.br

Author contributions

André L. S. Patriota: Methodology; Investigation; Data analysis/ plotting; Initial draft preparation; Filipe B. M. Barros: Investigation, Data curation; Visualization; Arnaldo M. P. Carneiro: Conceptualization, Supervision; Reviewing, Funding acquisition Pedro L. Guzzo: Conceptualization; Methodology, Writing, Reviewing, Editing; Data curation; Funding acquisition. All authors have read and agreed to the published version of the manuscript.